Influence of C, Mn and Ni Contents on Microstructure and Properties of Strong Steel Weld Metals — Part I. Effect of Nickel Content

E. Keehan*, L. Karlsson** and H.-O. Andrén*

* Department of Experimental Physics, Chalmers University of Technology, SE – 412 96 Gothenburg, Sweden.

** ESAB AB, P.O. Box 8004, SE–402 77 Gothenburg, Sweden.

Abstract

The effects of increasing nickel from 3 to 7 and 9 wt. % were investigated in high strength steel weld metals with 2 wt. % manganese. It was found that nickel additions were positive for strength but negative for impact toughness. Significant segregation of nickel and manganese to interdendritic regions was observed with the two higher nickel contents. In these weld metals a mainly martensitic microstructure developed at interdendritic regions while bainite was found at dendrite core regions. The microstructural inhomogeneity was due to segregation and the accompanying stabilisation of austenite in solute enriched regions to lower transformation temperatures. With 3 wt. % nickel the microstructure was found more homogenous with mainly bainite forming. The decrease in impact toughness with increasing nickel content was mainly attributed to the formation of coarse grained coalesced bainite.

Introduction

High strength steel with yield strength greater than 690 MPa (100 ksi) has been welded on a limited scale and with many precautions since the 1960's. Using mainly gas tungsten arc welding and tightly controlled conditions it proved possible to produce weld metals with both good strength and toughness. These weld metals have had limited use primarily due to economic factors and lack of flexibility. In recent years there has been a growing demand for high strength steels in such fields as construction, offshore and heavy engineering [1]. Given the very nature of these applications, welding must be flexibile, economical and mechanical properties must be insensitive to welding procedure. Shielded metal arc welding (SMAW), flux cored arc welding and submerged arc welding offer the flexibility and productivity required. However, with these methods toughness becomes problematic at low temperatures as strength levels increase.

Focusing on the SMAW method, current compositions utilised in high strength consumables are usually in the region 0.04–0.08C, 1–2Mn, 0.2–0.5Si, 1–3Ni wt. % along with minor additions of Cr, Mo and sometimes Cu [1–3]. From a review of literature on the role and effects of the individual alloying elements, nickel drew attention since it was reported to influence the stacking fault energy in such a manner that plastic deformation of ferrite at low temperatures is accommodated [4]. In addition it is known to add a solid solution hardening effect and to increase the hardenability, both promoting strength [5]. At larger concentrations it increases the preservation of retained austenite in the final microstructure.

In contrast, neural network modelling predicted that at manganese contents greater than 1.5 wt %, nickel additions lead to toughness loss, while below 1.5 wt %, nickel additions must take place in a controlled manner to have a positive effect of toughness [6]. Remarkably, when experimental weld metals were produced and the mechanical properties compared, it was found that the predictions were correct [6]. When weld metals studied in literature were compared, with nickel up to 7 wt. % and various Mn contents, they were also found to behave in agreement with the predictions [7–8].

When investigations of the 7 and 9 nickel weld metals were carried out using light optical microscopy (LOM), the microstructure was found to have fine scale morphology typical of martensite or bainite along with a novel constituent with large grain size [9]. Further studies with high resolution techniques on the 7 nickel weld metal revealed a lath-like microstructure of martensite at interdendritic regions along with mainly a mixture of upper, lower and a novel coarse grained bainite in dendrite core regions. The novel constituent was revealed to be that of coalesced bainite with an unusually large size [10]. The present paper is the first in a series of three papers dealing with the effects of nickel, manganese [11] and carbon [12] on high strength steel weld metals. This paper makes a comparison of the microstructure and properties of 7 and 9 Ni weld metals with those of a 3 Ni, 2 Mn, 0.5 Cr, 0.6 Mo, 0.05 C commercial electrode (ESAB OK 75.78).

Experimental Procedures

Welded joints were made according to ISO 2560 using 20 mm plates with a backing plate. The joints were buttered to limit dilution before the deposition of the experimental weld metals which took place in 33 cm runs with two or three runs per layer. The welding parameters utilised and chemical compositions are presented in Table 1. It was decided to call the experimental weld metals 7-2L250 and 9-2L250, where 7 or 9 was the Ni content in wt. %, 2 was Mn content in wt. %, L was low carbon (0.03 wt. %) and 250 was the interpass temperature in °C.

For Charpy testing, transverse specimens were machined having a cross section of 10×10×55 mm, notched perpendicular to the welding direction in the weld metal centre. Two or three specimens were tested at each temperature. Tensile specimens were machined longitudinally from

	OK 75.78	7-2L250	9-2L250
E / kJ mm^{-1}	1.4	1.2	1.2
IPT / °C	250	250	250
$t_{8/5}$ / s	13	12	11
C *	0.054	0.032	0.031
Mn	2.05	2.02	2.11
Ni	3.14	7.23	9.23
Cr	0.42	0.47	0.48
Si	0.26	0.25	0.27
P	0.009	0.011	0.011
Mo	0.6	0.63	0.64
Cu	0.01	0.03	0.03
S*	0.011	0.008	0.008
O / ppm*	300	380	340
N / ppm*	130	250	260

Table 1 Welding parameters and chemical composition. Welding parameters presented are energy input (E), interpass temperature (I.P.T.) and the estimated cooling time between 800 and 500 °C ($t_{8/5}$) calculated from WeldCalc [13]. Composition is in wt. % unless otherwise stated and '*' indicate elements analysed using Leco Combustion equipment.

the weld deposits with a specimen diameter of 10 mm and a gauge length of 70 mm. Charpy impact testing and tensile testing were performed in compliance with standard EN 10045–1.

Specimens for metallographic analysis from the weld metal cross section, perpendicular to the welding direction, were mounted in bakelite, wet ground and polished to 1 μm diamond grain size. Polished samples were examined with scanning electron microscopy (SEM) while etched specimens using 2 % nital were studied using both LOM and field emission gun scanning electron microscopy (FEGSEM). A Leitz Aristomet LOM, a Philips XL30 SEM and a Leo Ultra 55 FEGSEM were used in these examinations.

For transmission electron microscopy (TEM) studies, 3 mm disc shape specimens perpendicular to the welding direction were wet ground to between 50 and 80 μm in thickness. The discs were then jet electropolished at –35 °C using 10 % perchloric acid in methanol. After electropolishing, the samples (which contained a small hole with thin areas around it) were further thinned by ion beam milling for a few minutes at a low angle using a Gatan Precision Ion Polishing System (PIPS). These specimens were examined with a Jeol 2000 FX TEM and a Philips CM 200 TEM.

Hollow and solid cylindrical dilatometry specimens were machined from the centre of the welded joint. Hollow specimens with an outer diameter of 4.9 mm, inner diameter of 3.5 mm and length of 12.5 mm were used for measurements with cooling rates greater that 50 °C / s while solid specimens with 3 mm diameter and 10 mm length were used for lower cooling rates. All specimens were analysed using a Theta Dilatronic III dilatometer to record phase transformation temperatures. The specimens were heated up to 1000 °C at a rate of 25°C / s, held for 5

minutes and then cooled at different rates to room temperature. Individual samples were used for each cooling rate.

Results

Mechanical Properties

It was found that Ni additions were positive for strength but negative for toughness as predicted by the neural network modelling. Figure 1 shows that OK 75.78 with the lowest Ni content (3 wt. %) had the best impact toughness both at room temperature and at –40 °C where it recorded 81 J and 51 J, respectively. A progressive loss of toughness was experienced as the nickel content increased to 7 and then 9 wt. %. For the 9 Ni weld metal only 12 J was recorded at –40 °C and 16 J at room temperature. In Table 2 it is seen that Ni additions were positive for strength. Looking first at OK 75.58 with 3 wt. % Ni, it recorded 756 MPa in yield strength and 945 MPa in ultimate tensile strength. The best tensile results were achieved with the 9 Ni weld metal where a yield of 848 MPa and a tensile strength of 1051 MPa was recorded. Also it should be noted that both these latter alloys have a slightly lower carbon content than OK 75.78.

	OK 75.78	7-2L250	9-2L250
YS / MPa	756	795	848
UTS / MPa	945	1006	1051
YS / UTS	0.8	0.79	0.81
A_5 / %	19.4	14.8	13.1

Table 2 Tensile properties of the weld metals.

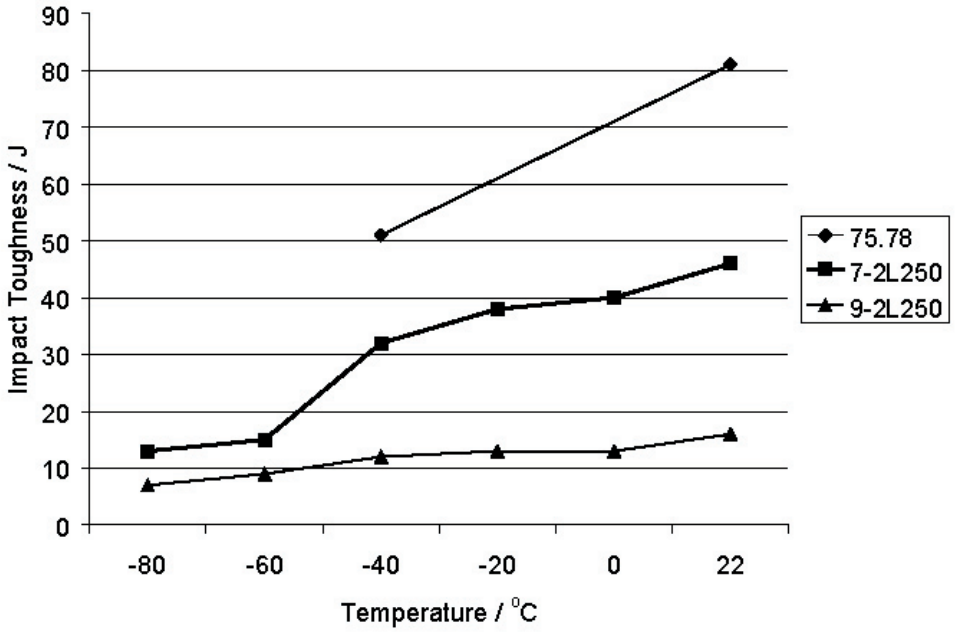

Figure 1 Charpy–V impact toughness for the weld metals.

Microstructure – Last bead

The microstructure of OK 75.78 has previously been characterised and it was found to consist of a mixture of martensite and bainite with the percentage of each directly related to the welding parameters [14–15]. Given these conclusions, it was decided for the purpose of completeness to characterise the microstructure obtained for the given welding parameters using LOM and FEGSEM.

Microstructural investigations were first carried out on the as deposited last bead. LOM micrographs from the three weld metals are presented in Figure 2. In the experimental weld metals traces of the former dendritic structure that developed during solidification were clearly seen. In work presented elsewhere this was explained by the fact that the experimental weld metals with greater Ni content solidify as austenite while OK 75.78 solidifies primarily as δ–ferrite [14]. Overall it was concluded that a fine scale microstructure developed which was believed to be a mixture of martensite or bainite and characterisation tools with higher resolution were required to make a complete interpretation.

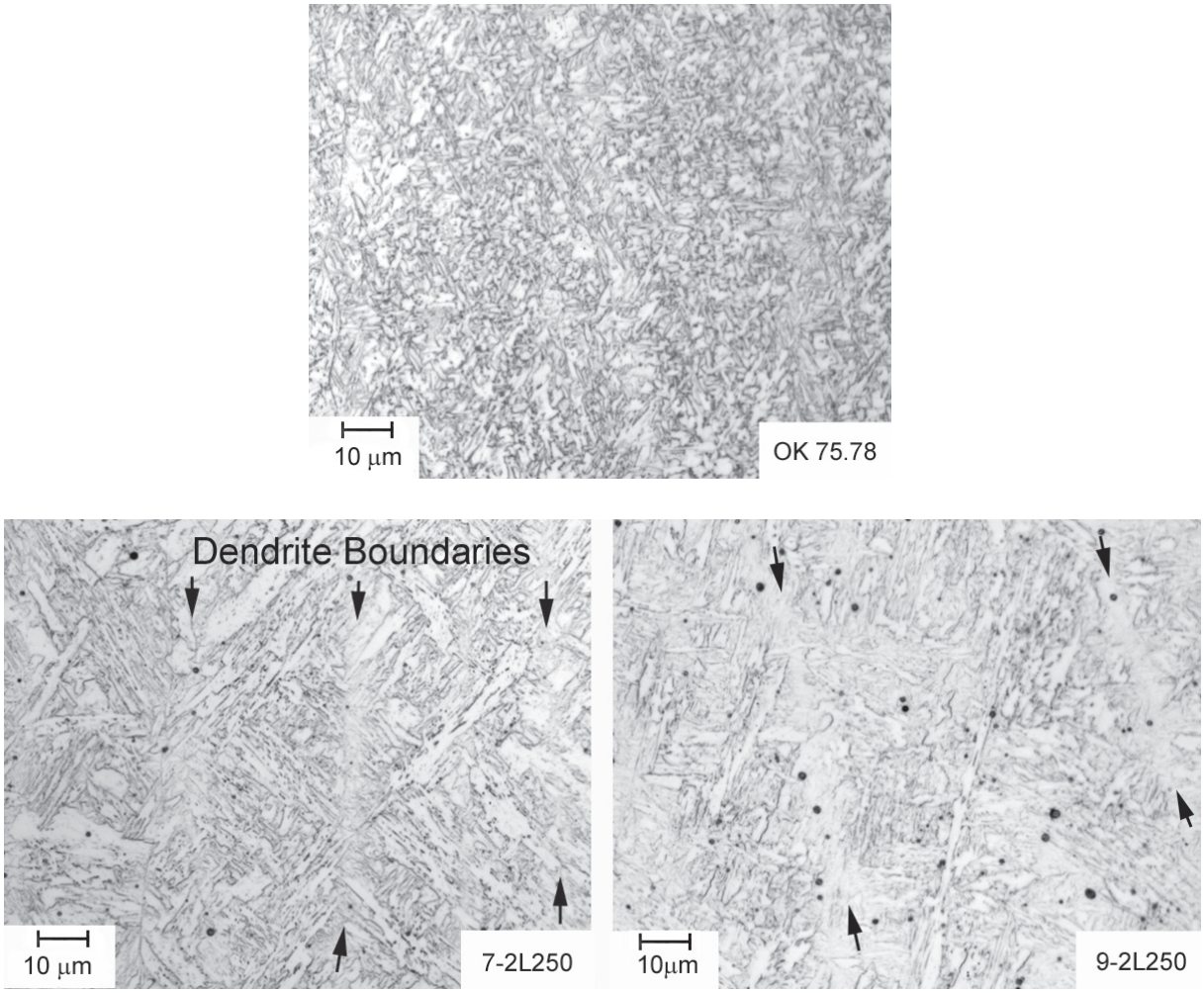

Figure 2 LOM micrographs from the last bead of weld deposited with the commercial electrode OK 75.78 and experimental weld metals 7-2L250 and 9-2L250.

Investigations with FEGSEM were found to be very revealing. Micrographs from OK 75.78 weld metal are presented in Figures 3–5. An overview of the microstructure is presented in Figure 3 and from investigations at higher magnification it was found the microstructure was mainly bainitic. In Figure 4 it can be observed that films developed at the bainitic ferrite plate boundaries. In Figure 5 at very high magnification, precipitates were also found within the plates.

FEGSEM micrographs from the experimental weld metals are presented in Figures 6–9. It was found that both these weld metals were similar to each other and there were noticeable differences from the OK 75.78 weld metal. With FEGSEM it was again possible to see the former dendrite boundaries that developed during solidification. Low magnification micrographs giving overviews of the microstructure in both weld metals are shown in Figures 6 and 7. In both micrographs it can be seen that a finer morphology formed at the interdendritic regions. Figure 8 shows a representative micrograph of a former interdendritic region at higher magnification in weld metal 7-2L250. In this region the microstructure was mainly that of martensite. Some distance from the boundary, upper bainite can also be observed in the micrograph. In dendrite core regions, large grains several microns in size can be observed (Figure 6 and 7). In previous work [10] on 7-2L250, these large grains were characterised to be a special form of bainite with a large grain size forming when B_S is very close to M_S. This type of bainite is called coa-

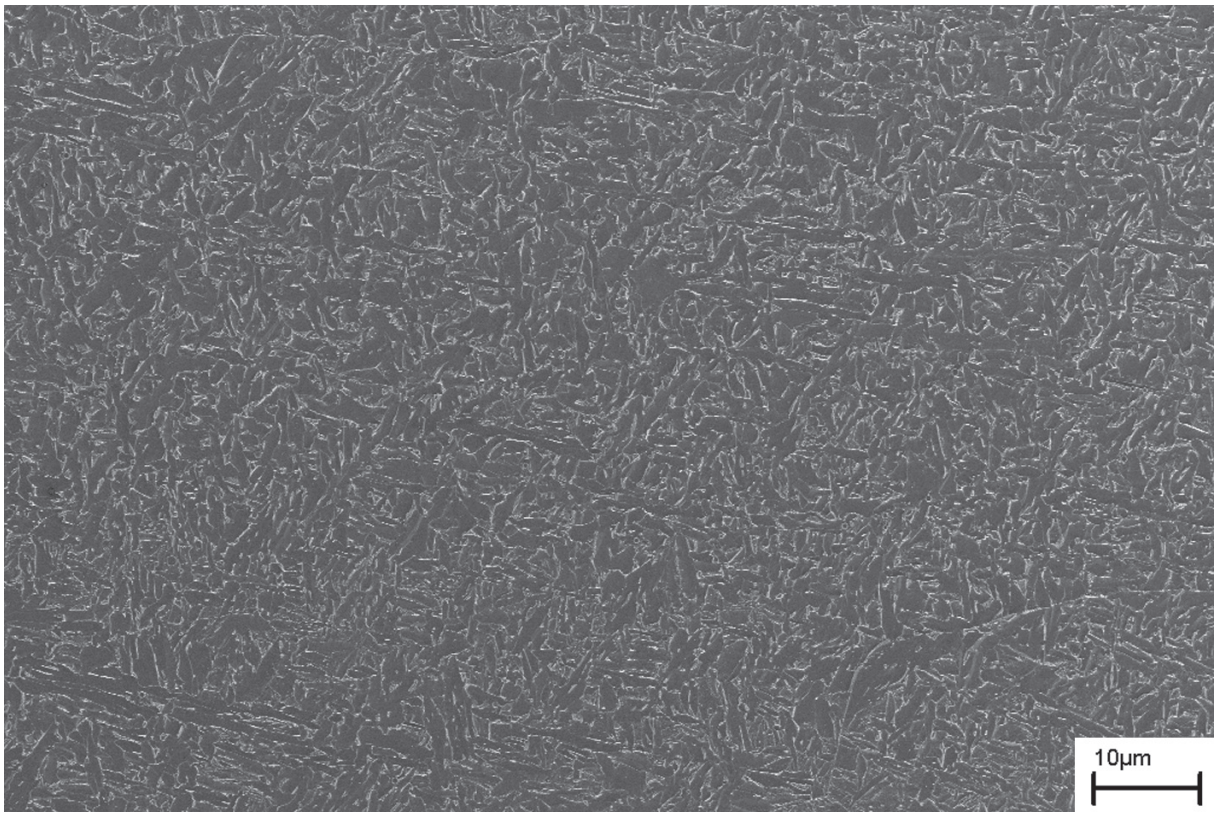

Figure 3 FEGSEM micrograph of weld metal deposited with OK 75.78 giving an overview of the microstructure in the last bead.

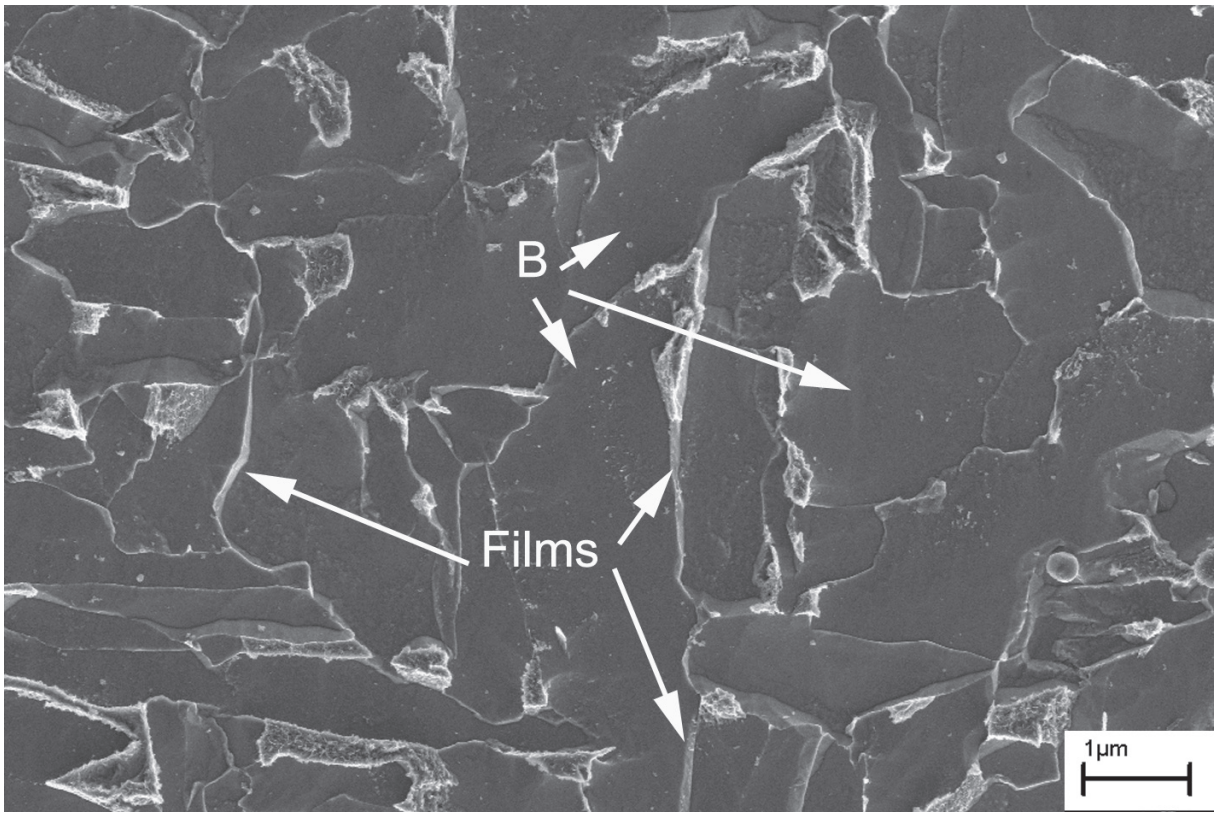

Figure 4 FEGSEM image confirming that the microstructure is mainly bainitic (B) in the last bead of OK 75.78 weld metal. Films are also observed at the bainitic ferrite boundaries.

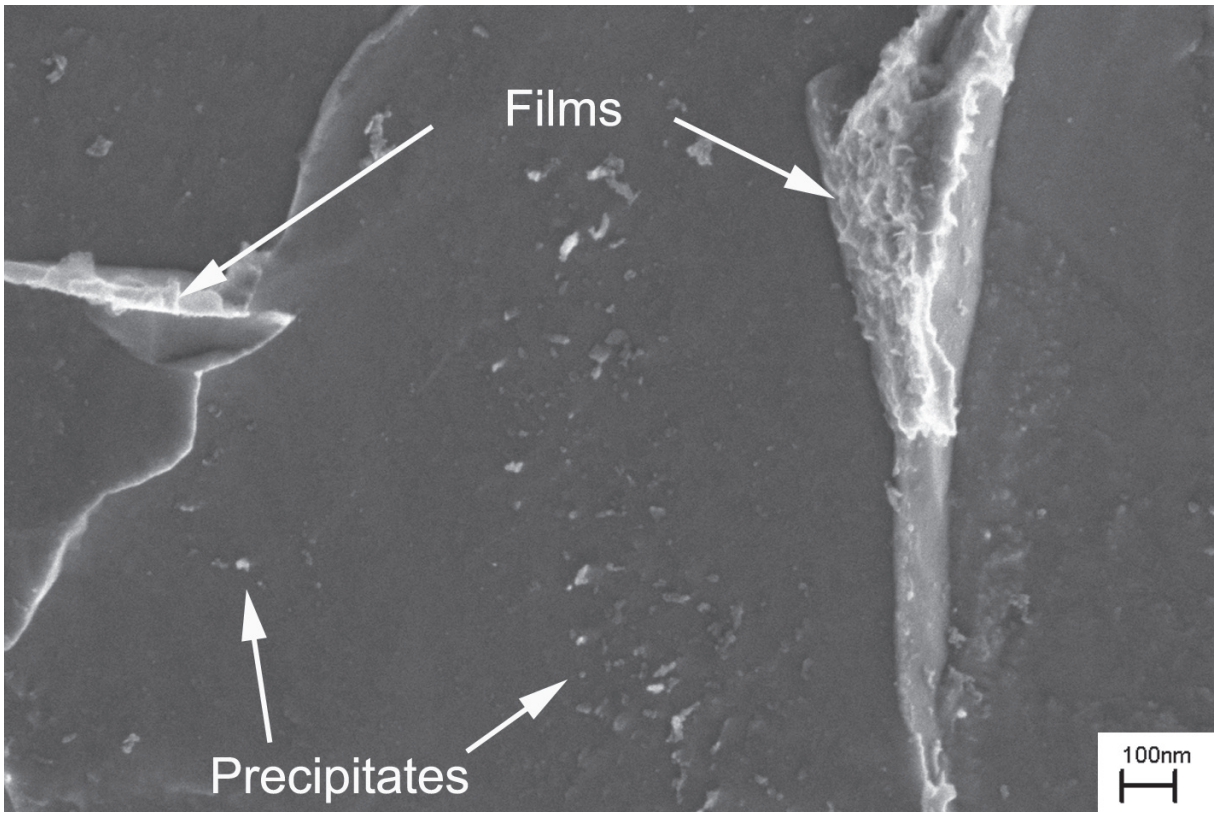

Figure 5 High magnification FEGSEM micrograph showing precipitates within bainitic ferrite and films at the boundaries in the last bead of OK 75.78 weld metal.

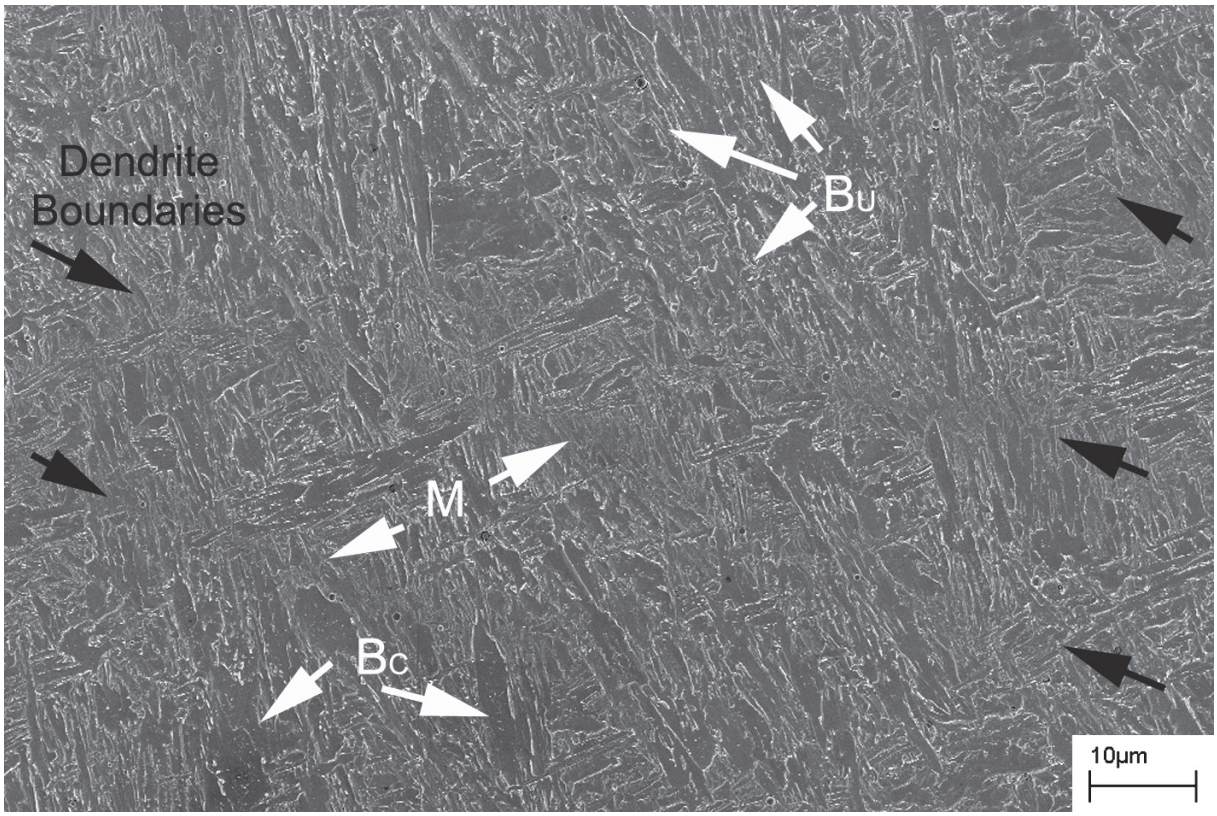

Figure 6 The last bead in 7-2L250 having a mixture of martensite (M) coalesced bainite (B_C) and upper bainite (B_U) as shown with FEGSEM.

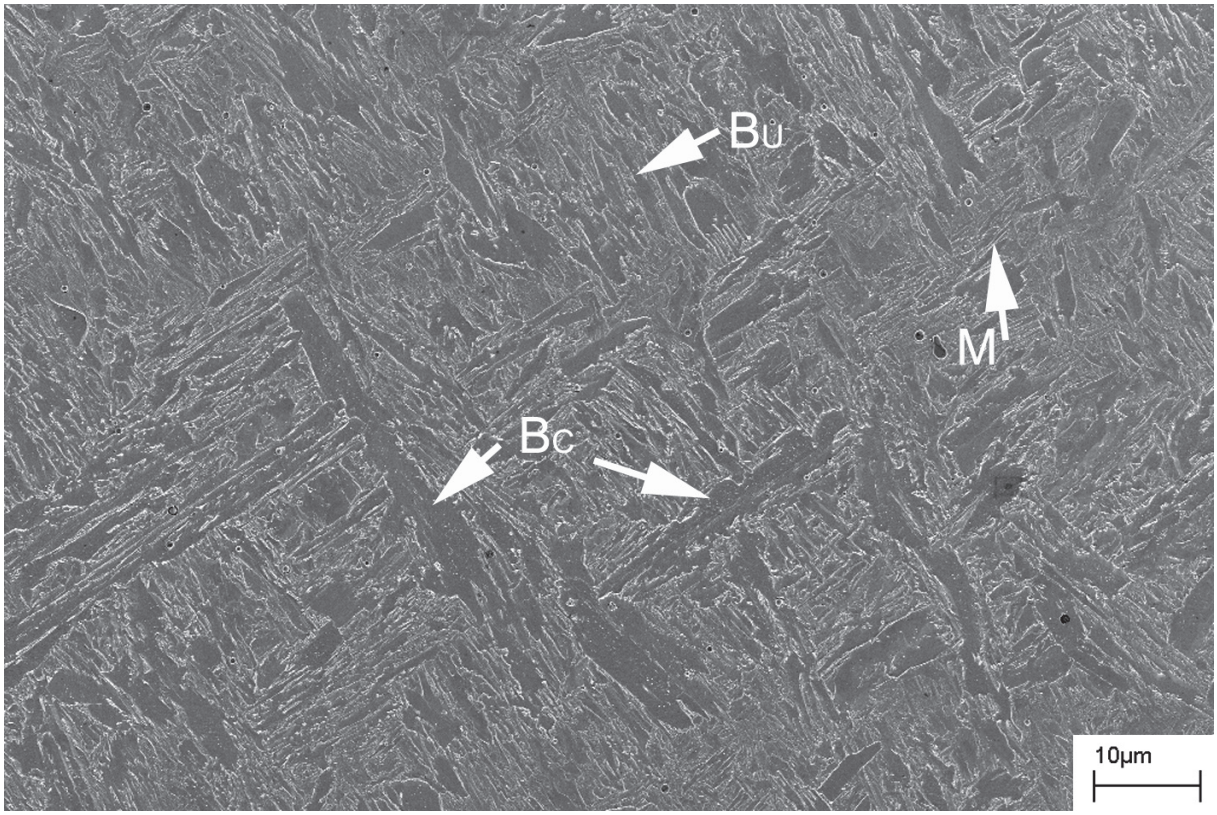

Figure 7 FEGSEM micrograph of the last bead in 9-2L250 showing mainly martensite (M) at interdendriticc regions along with coalesced lower bainite (B_C) and upper bainite (B_U) at dendrite core regions.

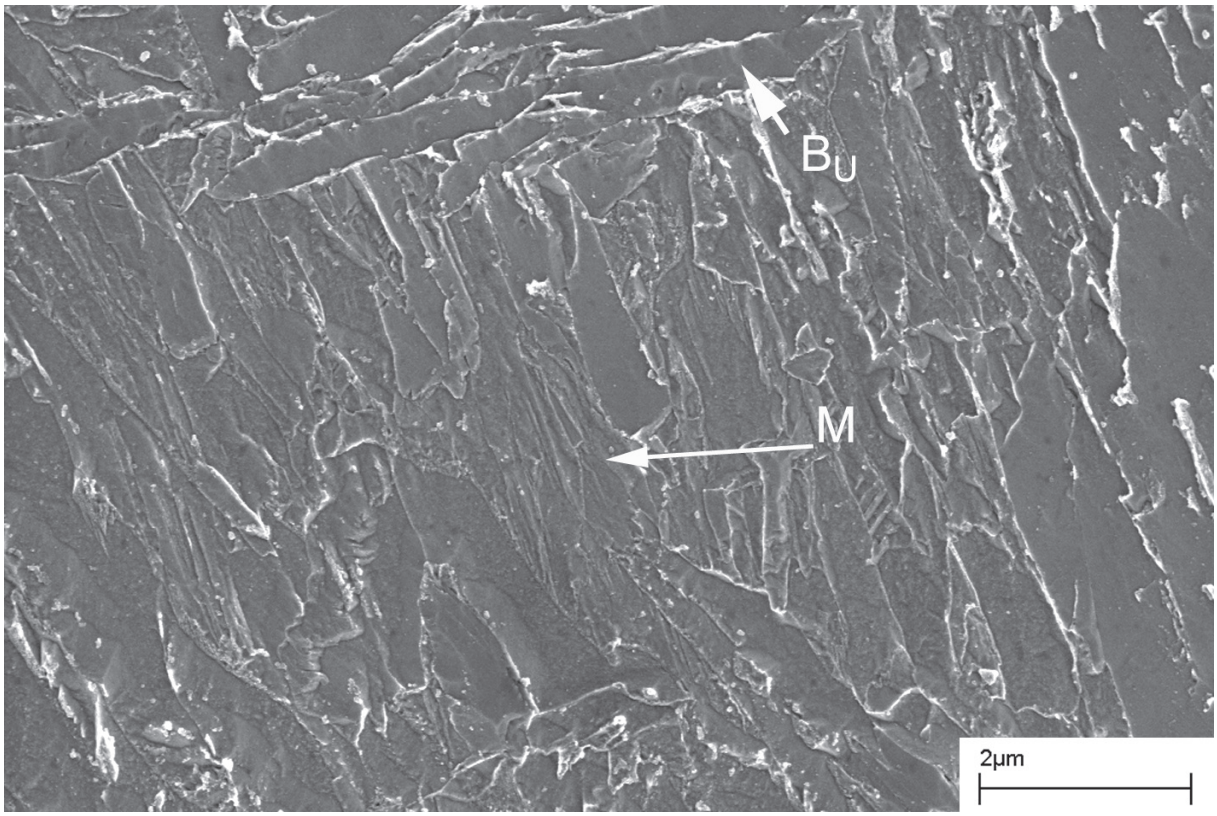

Figure 8 Interdendritic region in the last bead of 7-2L250 at high magnification showing mainly martensite (M) at the former dendrite boundary. Upper bainite (B_U) is also seen within the micrograph.

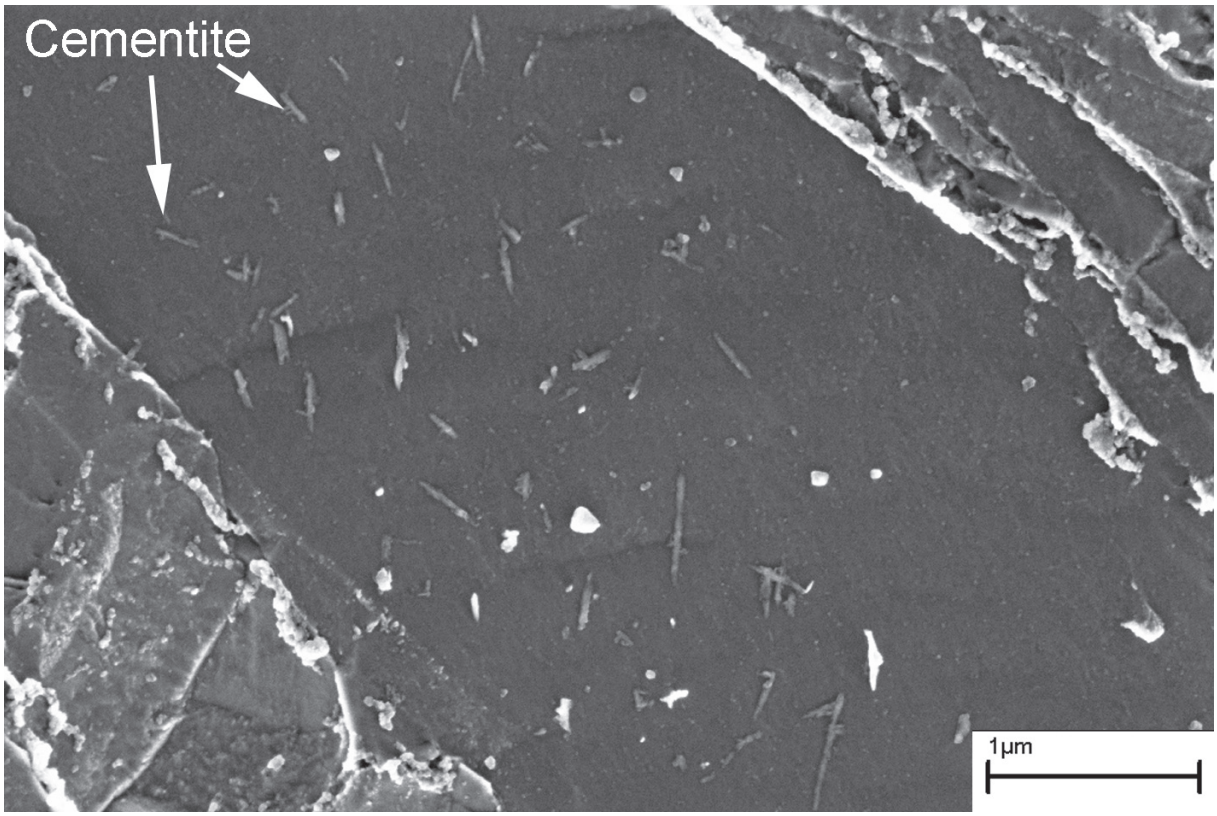

Figure 9 Higher magnification FEGSEM micrograph showing precipitation within a bainitic ferrite plate in 9-2L250.

lesced bainite. Figure 9 shows bainitic ferrite in weld metal 9-2L250 at high magnification. It was observed that precipitates formed within the bainitic ferrite. Some of these precipitates are deemed to be that of cementite where since precipitates of similar size and morphology were characterised with TEM in Paper two of this series [10].

Elemental Distribution

Investigations on polished samples with SEM in the backscattered mode gave a clear contrast between the dendrite boundaries and the dendrite core regions in the last bead of the experimental weld metals. EDX line scans were made across the dendrites and the results are plotted in Figure 10. It is seen that the concentrations follow a wave-like pattern with segregation of Mn and Ni reaching a maximum concentration at the dendrite boundaries. The degree of segregation was quantified using spot analysis and between five and ten examinations were carried out in both the dendrite core regions and in the interdendritic regions. The results presented in Table 3 are the average values recorded in each region. Despite the overestimation of Mn, the results allow a clear comparison and a clear estimation of the degree of segregation between the dendrite boundaries and centres. Weld metal 9-2L250 recorded the greatest difference between the two regions with a difference of 1.15 wt. % for Mn and 2.6 wt. % for Ni.

Weld Metal	Mn	Ni
7-2L250 Boun.	3.10	8.18
7-2L250 Cent.	2.35	6.30
7-2L250 Diff.	0.75	1.88
9-2L250 Boun.	3.20	10.30
9-2L250 Cent.	2.05	7.70
9-2L250 Diff.	1.15	2.60

Table 3 Average compositions recorded in wt. % at dendrite boundary regions (Boun) and dendrite centre (Cent) in the last bead using EDX spot analysis.

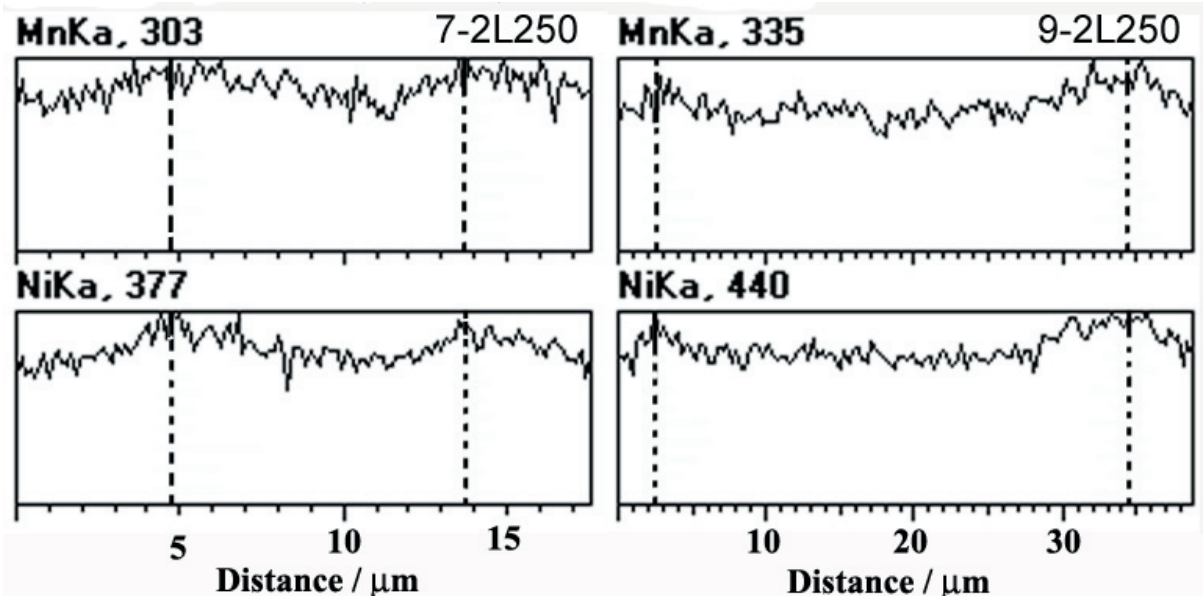

Figure 10 EDX line scans across dendrites in the last bead of 7-2L250 and 9-2L250 showing segregation of Ni and Mn to interdendritic regions (indicated by broken lines).

Microstructure — Reheated Beads

FEGSEM micrographs from the centre of a reheated bead in OK 75.78 weld metal are presented in Figures 11–13. After reheating, traces of the former dendrite structure could be observed to a limited degree in Figure 11. Mainly tempered martensite was found at the former interdendritic regions with tempered bainite at dendrite core regions. The morphology of the individual constituents is shown at higher magnification in Figures 12 and 13.

The reheated microstructure of the experimental weld metals were also examined with FEGSEM and some micrographs are presented in Figures 14 – 16. An overview of the microstructure in 7-2L250 is shown in Figures 14. It was generally found that the microstructure consisted of tempered martensite in dendrite boundary regions (Figure 15) and tempered bainite in the centre of the dendrites (Figure 16). The location of the cementite within the microstructure shown in Figure 16 was interpreted from the understanding obtained with TEM investigations [10].

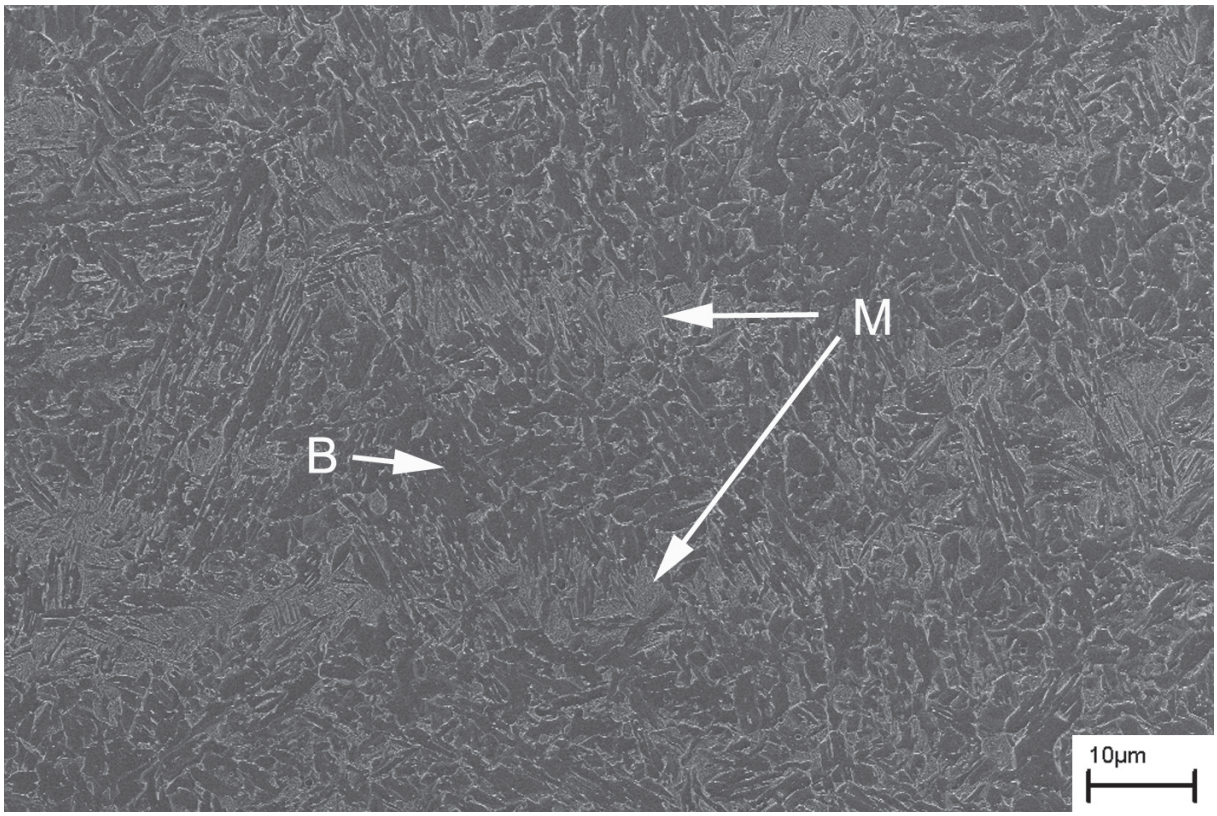

Figure 11 A FEGSEM overview showing the microstructure in the centre of a reheated OK 75.78 weld bead. Tempered martensite (M) is mainly found at the dendrite boundary regions and bainite (B) in the centre of the dendrites.

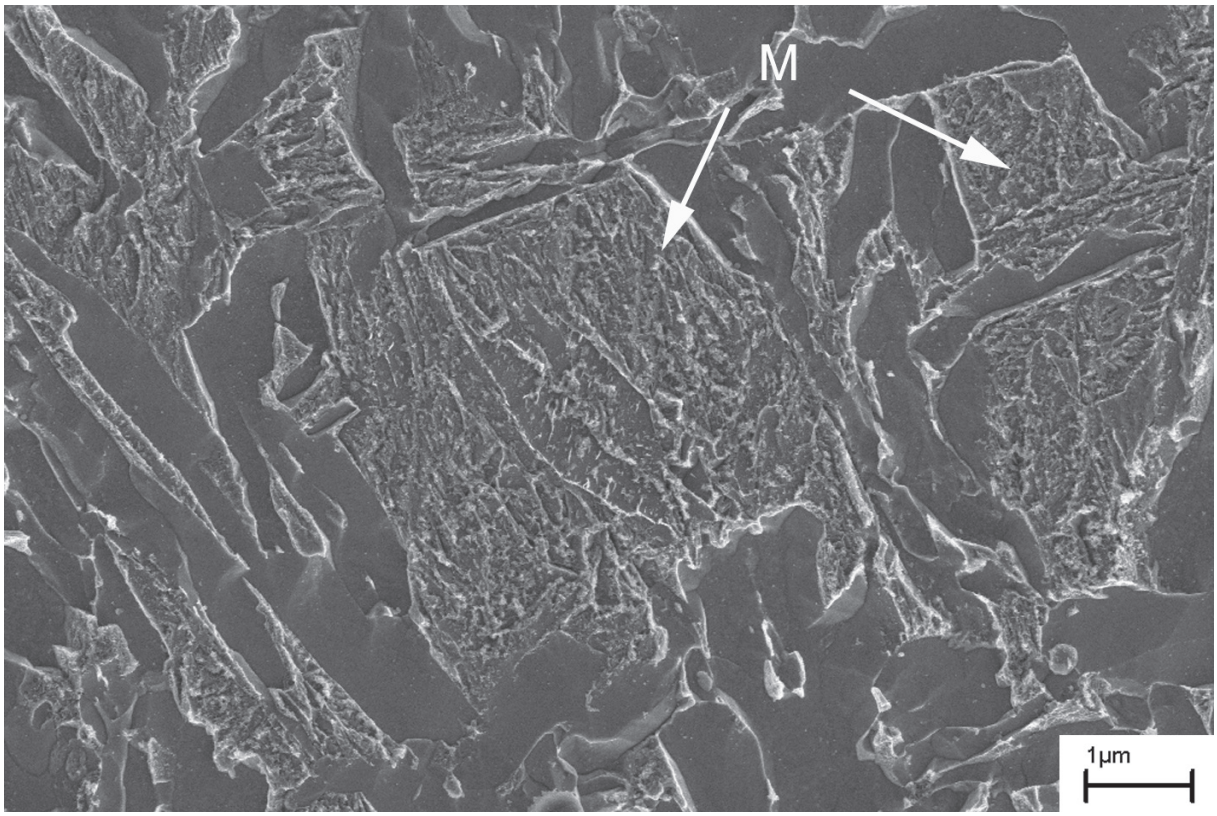

Figure 12 Mainly tempered martensite (M) in an interdendritic region in the centre of a reheated OK 75.78 weld bead shown using FEGSEM.

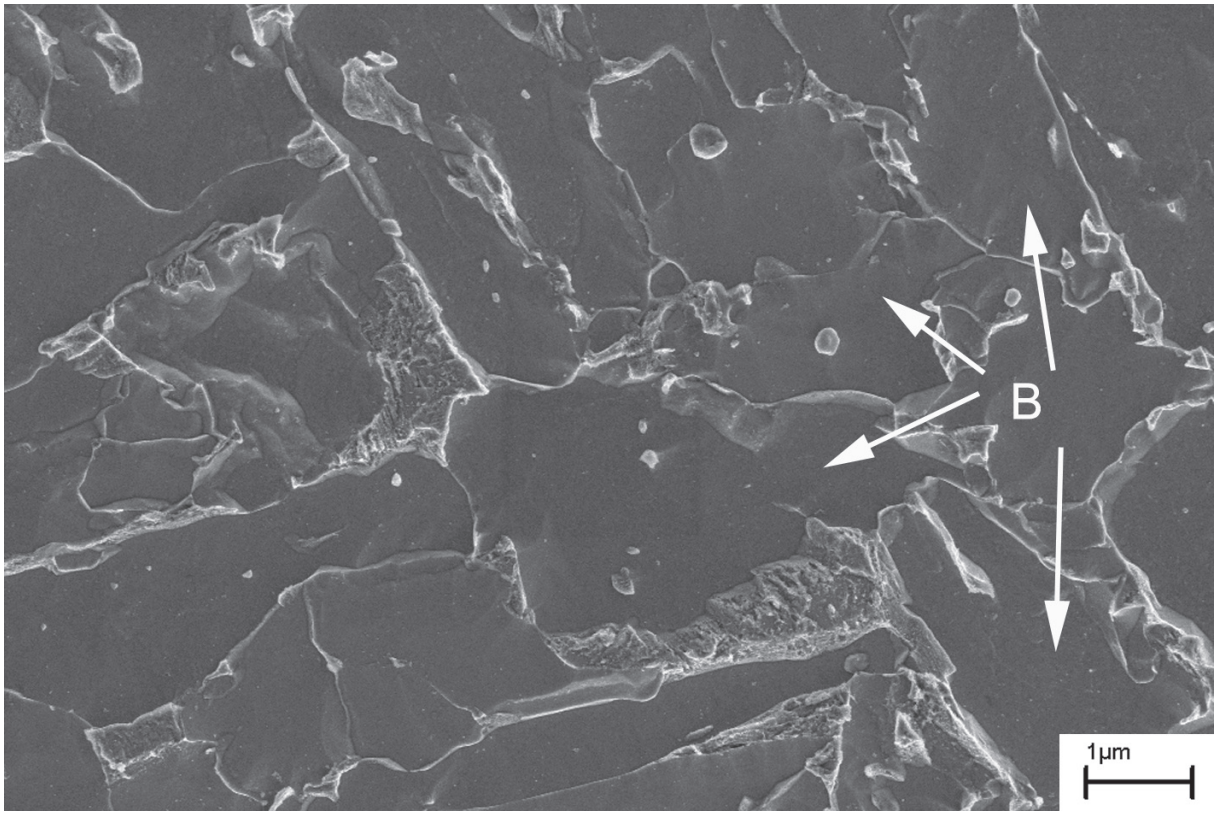

Figure 13 FEGSEM micrograph showing mainly tempered bainite (B) in the centre of a reheated bead in OK 75.78.

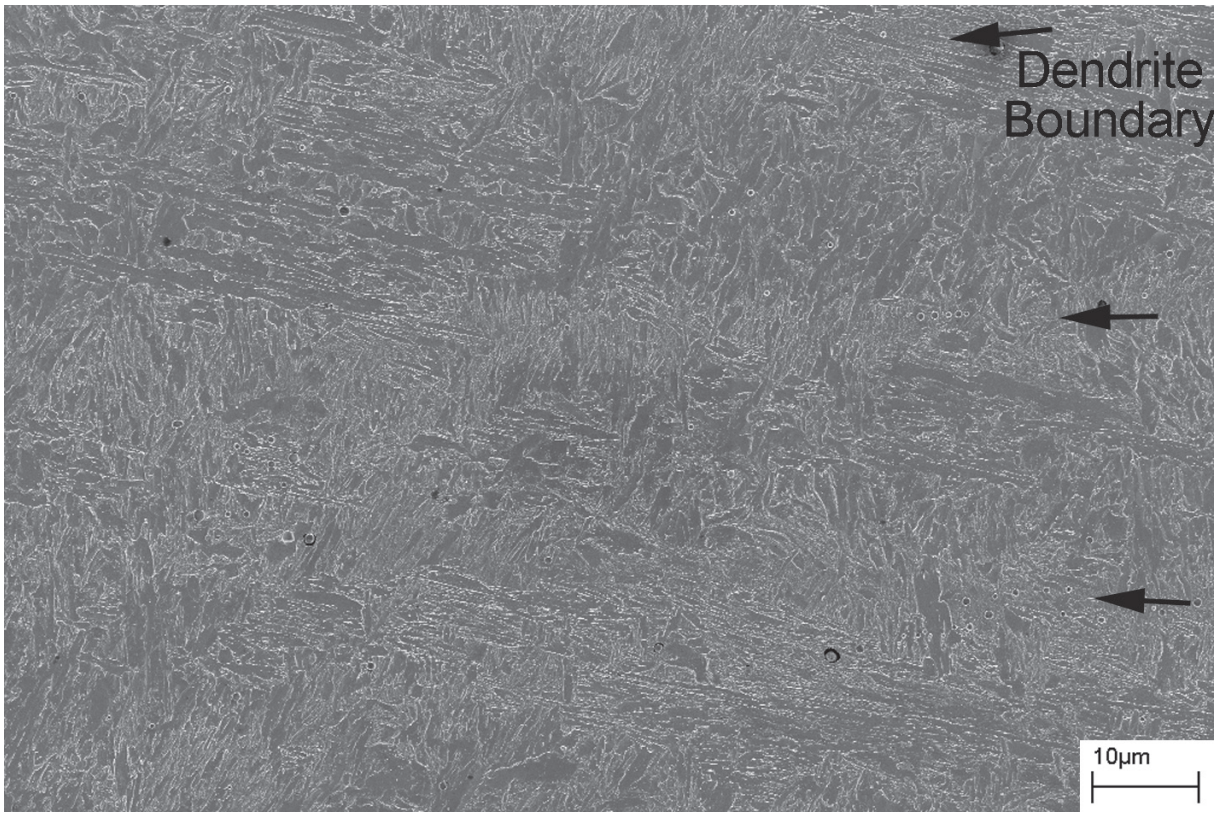

Figure 14 Overview showing the centre of a reheated bead in 7-2L250.

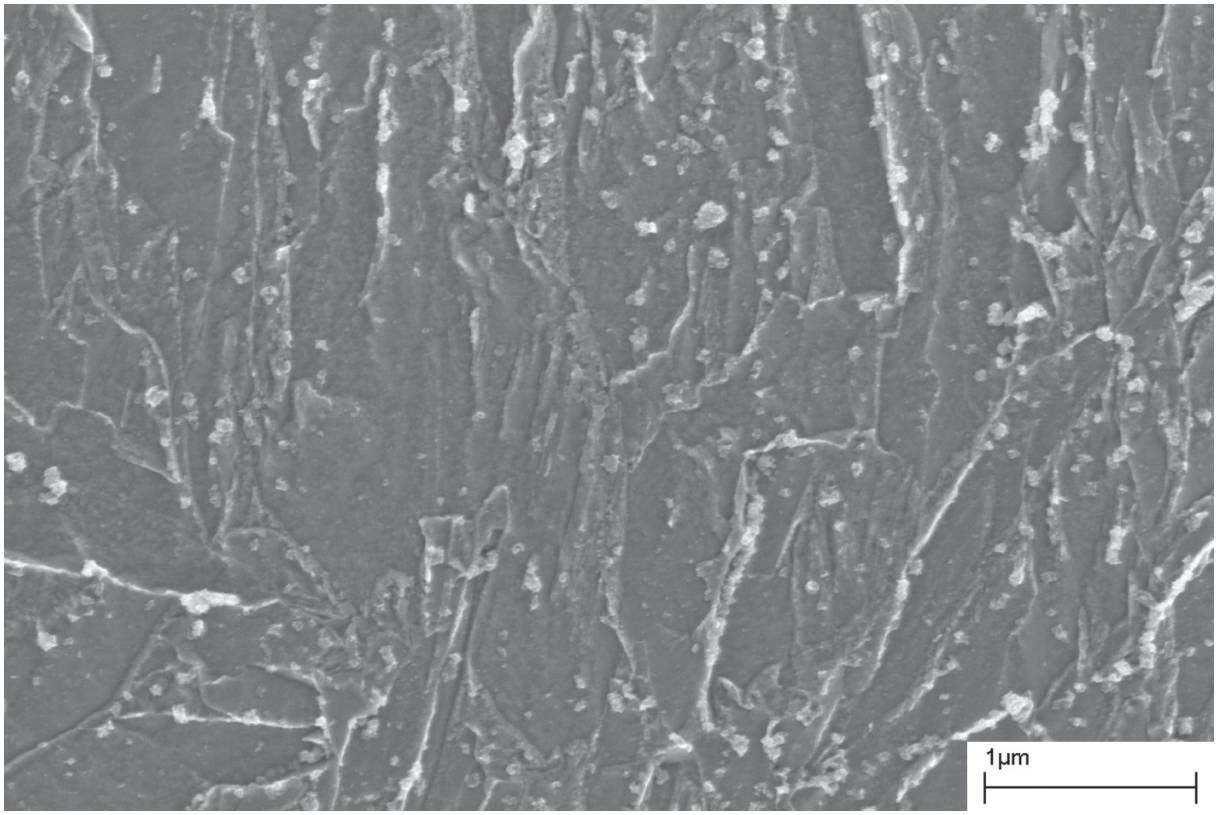

Figure 15 High magnification FEGSEM micrograph of an interdendritic region showing the general appearance of mainly tempered martensite in a reheated weld bead of 7-2L250. Some tempered bainite can also be seen.

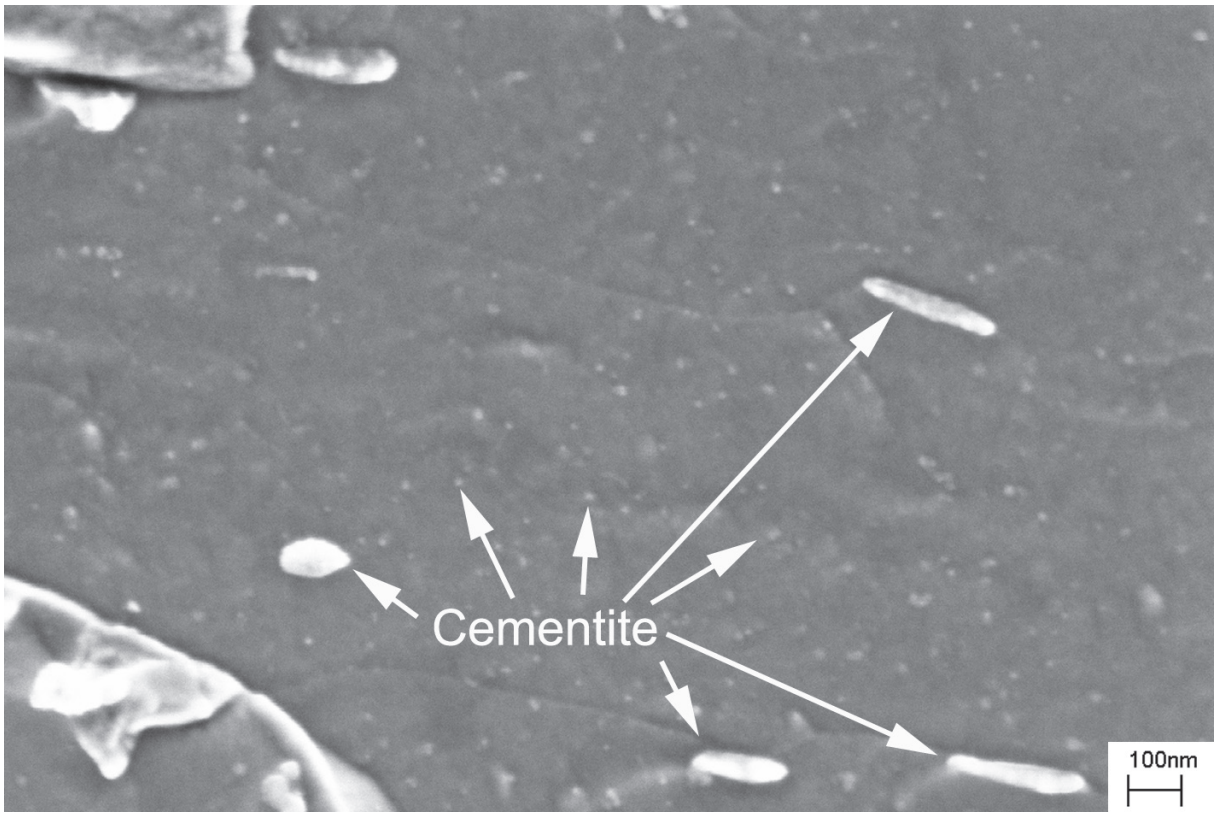

Figure 16 FEGSEM micrograph showing the redistribution of carbon in bainitic ferrite after reheating in a dendrite core region of 7-2L250. Interpretations that the large and small precipitates are cementite were made from investigations with TEM.

Investigations with TEM were carried out on reheated beads of both 7-2L250 and 9-2L250. Results from 9-2L250 are presented in Figures 17 and 18 while limited results from 7-2L250 are presented in previous work [10]. Figure 17 shows a bright and dark field image with a corresponding selected area diffraction pattern from weld metal 9-2L250. The reflections in the diffraction pattern were found to correspond to both ferrite and cementite [17–19]. When a cementite reflection was chosen to form a dark field image it was seen that very small precipitates (<15 nm) in the bright field image were illuminated. A low magnification bright and dark field image of the same area showing cementite at lath boundaries is presented in Figure 18.

Dilatometry

Phase transformation temperatures were measured using dilatometry. It was found that Ac_1 and Ac_3 were at 665 °C and 720 °C respectively for 9-2L250 when samples were heated at a rate of 25 °C / s from room temperature. These can be compared to 690 °C and 740 °C for Ac_1 and Ac_3 for 7-2L250.

Austenite began transformation in the region of 365 °C when cooled at a rate of approximately 30 °C / s as well as at 1 °C / s for weld metal 9-2L250. With 7 wt % nickel, transformation temperatures were slightly higher with 373 °C and 390 °C recorded at cooling rates of 25°C / s and 1 °C / s, respectively.

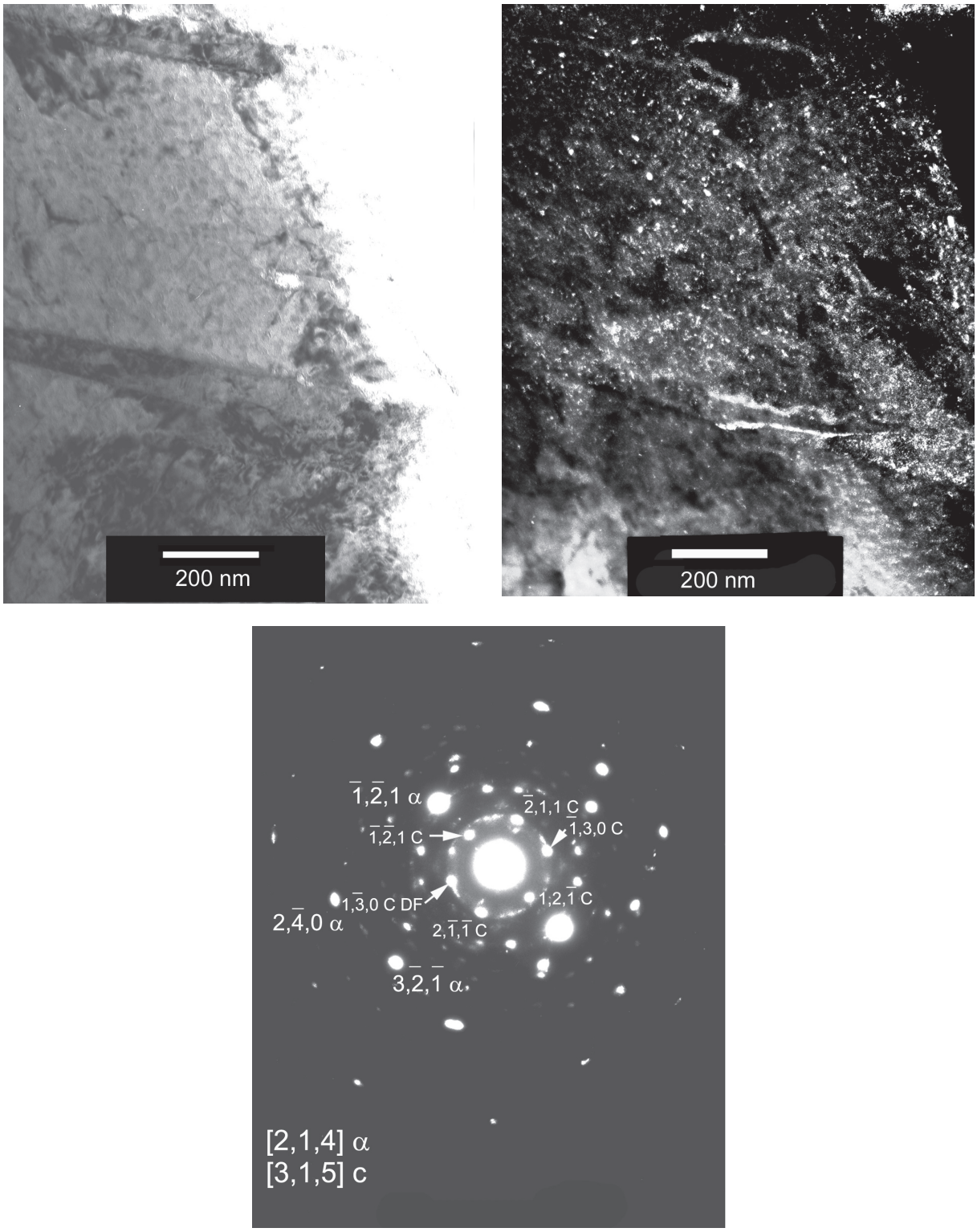

Figure 17 Bright and dark field images with corresponding SAED pattern of cementite obtained from the centre of a reheated bead in weld metal 9-2L250. The dark field image was formed using the {1,–3,0} C reflection in the corresponding SAED.

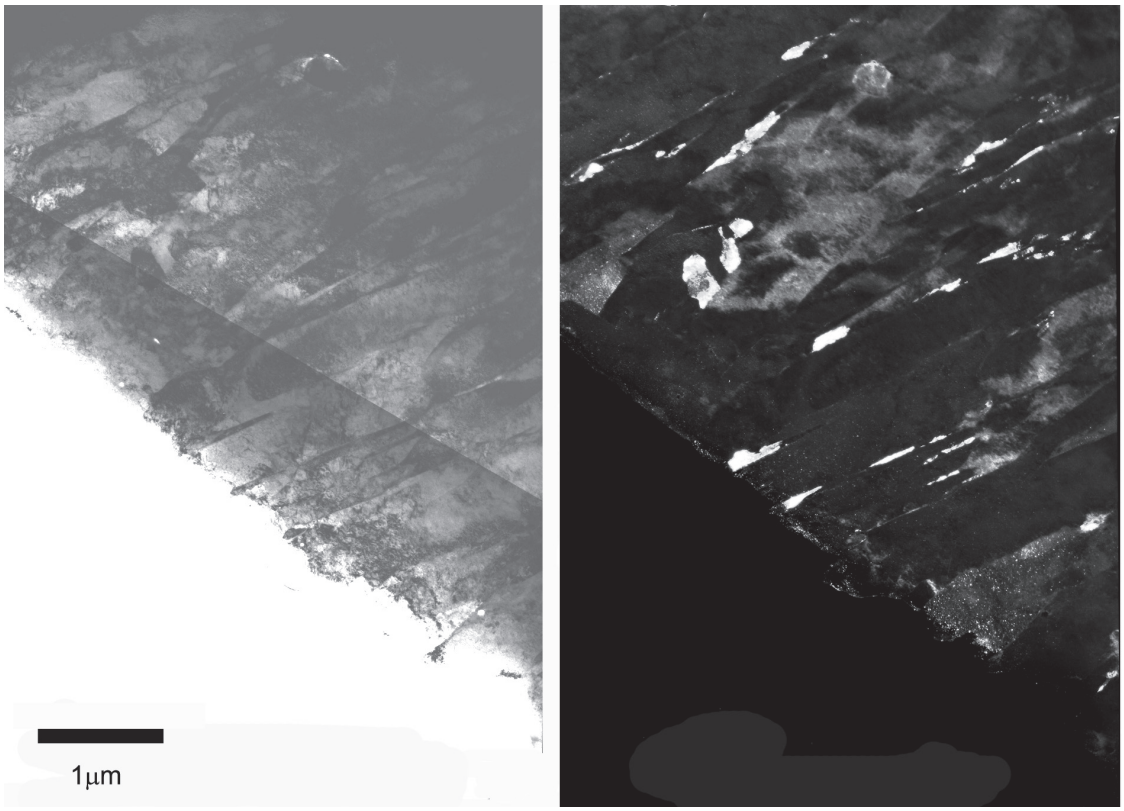

Figure 18 Bright and dark field images of cementite at lath boundaries in the centre of a re-heated bead in weld metal 9-2L250.

Discussion

In this work it was found that Ni additions were positive for strength but negative for toughness at a Mn level of 2 wt. %. The nickel content, its interaction with other alloying elements, segregation and its effect on transformation temperature all have a major role to play. Ultimately it determines what phases and constituents develop during solidification and cooling which in turn govern the mechanical properties.

From microscopy it was found that the overall microstructure was very fine in the 7 and 9 wt. % Ni weld metals. With a combination of both FEGSEM and TEM a mixture of bainite, martensite and films of retained austenite [10] were observed. It is concluded from thermodynamic modelling [9] that these weld metals solidify as austenite resulting in significant segregation. In both weld metals, segregation of nickel and manganese to interdendritic regions was observed and quantified using EDX analysis (Table 3). These local differences in alloying content are believed to cause the microstructural differences across the dendrites. Dilatometry measurements showed that both Ni and Mn [18] stabilise austenite to lower transformation temperatures. In agreement with this coalesced bainite and upper bainite were mainly found in dendrite core regions while martensite was found predominantly at interdendritic regions (Figures 6 and 7).

In regions reheated due to multiple weld passes the microstructure consisted of a mixture of tempered bainite (Figure 15) and tempered martensite (Figure 16). Overall there was no remarkable difference between the microstructure of 7-2L250 and 9-2L250. Coarsening and spheroidising of cementite was seen and very numerous small precipitates were also found to form. These precipitates most likely developed from the carbon dissolved on reheating to temperatures close to or above Ac_1.

As expected nickel additions were found to stabilise austenite. Minor differences were observed in Ac_1 and Ac_3 temperatures between the 7 and 9 wt. % nickel weld metals with transformation to austenite taking place at lower temperatures for 9-2L250. Maybe more importantly transformation of austenite took place at lower temperatures.

In contrast to the experimental weld metals, OK 75.78 was found to be mainly bainitic in nature in the as-deposited last bead. This weld metal solidifies predominantly as δ-ferrite [15] and as a result segregation was not as pronounced. Precipitates were observed within the bainitic ferrite and films were found at the boundaries (Figure 5). Overall the microstructure was more homogeneous in its morphology (Figures 2 and 3) and there was the notable absence of coalesced bainite. In reheated regions, OK 75.78 had many similarities to the experimental weld metals but there were also some differences. Similar to the experimental weld metals, OK 75.78 formed some martensite at interdendritic regions and bainite within the dendrites. However it was noted that the grain size in these regions was finer than in the experimental weld metals.

The loss of toughness experienced with nickel additions can be attributed mainly to the larger effective grain size developed within the microstructure. Increasing nickel stabilised austenite to lower transformation temperatures and promoted the formation of coarse grained coalesced bainite and martensite. The extra strength is most likely due to the combination of solid solution hardening attained from nickel and the greater amounts of martensite present within the microstructure. A more detailed discussion of mechanical properties can be found elsewhere [16]

Conclusions

The effect of nickel additions on microstructural and mechanical properties were investigated in high strength steel weld metals. Using the composition of the SMAW electrode OK 75.78 as the basis for research, nickel was increased from 3 to 7 and 9 wt. %.

Nickel additions stabilised austenite to lower transformation temperatures. Greater amounts of martensite and coalesced bainite were formed as nickel increased. Segregation of Ni and Mn to interdendritic regions leads to greater amounts of martensite forming at interdendritic regions and more bainite at dendrite core regions.

Ni additions were positive for strength but negative for toughness. Solid solution hardening due to nickel additions and greater amounts of martensite increased strength. The toughness loss was mainly due to the formation of coarse grained coalesced bainite

Acknowledgements

Prof. L.-E. Svensson of Chalmers University of Technology and Prof. H. K. D. H. Bhadeshia of the University of Cambridge is thanked for fruitful discussions. ESAB AB is thanked for the production of experimental weld metals, permission to publish results and financial support. Knowledge foundation of Sweden is thanked for additional financial support.

Reference

1. D.J. Widgery, L. Karlsson, M. Murugananth and E. Keehan, Approaches to the development of high strength weld metals, Proceedings 2nd Int. Symposium on High Strength Steel, Norway 2002.
2. W. Wang and S. Liu, Welding Journal, July 2002, p. s–132.
3. D.P. Fairchild, M.L. Macia, N.V. Bangaru and J.Y. Koo, Proc. 13th Int. Offshore and Polar Eng. Conf., Honolulu, Hawaii, USA, May 25–30, 2003, p. 26.
4. L.-E. Svensson, Control of microstructure and properties in steel arc welds, CRC Press, Inc., 1994
5. ASM International, Weld Integrity and Performance, S. Lampman Tech. Ed., 1997.
6. M. Murugananth, H. K. D. H. Bhadeshia, E. Keehan, H. O. Andrén, L. Karlsson, Strong and Tough Ferritic Steel Welds, Proc. 6th Int. Seminar, "Numerical Analysis of Weldability", Austria (2001)
7. Y. Kang, H.J. Kim, and S.K. Hwang, ISIJ International (Japan), 40 December (2000), p. 1237.
8. Zhang Z, Farrar RA, Influence of Mn and Ni on the microstructure and toughness of C–Mn–Ni weld metals, Welding Journal 76 : (5) S183–S196 May1997
9. E. Keehan, L. Karlsson, H.-O. Andrén, L.-E. Svensson, New developments with C–Mn–Ni high strength steel weld metals, Part A. Microstructure, In Manuscript
10. E. Keehan, H. K. D. H. Bhadeshia, H.-O. Andrén, L. Karlsson, L.-E. Svensson, Micro structure characterisation of a high strength steel weld metal containing the novel con stituent coalesced bainite, In manuscript
11. E. Keehan, L. Karlsson, H.-O. Andrén, H. K. D. H. Bhadeshia, Influence of C, Mn and Ni contents on microstructure and properties of strong steel weld metals, Part II. Impact toughness gain from manganese reductions, In manuscript
12. E. Keehan, L. Karlsson, H.-O. Andrén, H. K. D. H. Bhadeshia, Influence of C, Mn and Ni contents on microstructure and properties of strong steel weld metals, Part III. Increased strength from carbon additions, In manuscript
13. SSAB Oxelösund, WeldCalc, Version 1.0.0, 98 – 99

14. M. Lord, Welding in the world, 41 (1998) p.452
15. M. Lord: Design and Modelling of Ultra – High Strength Steel Weld Deposits, Ph. D. Thesis, (1999), University of Cambridge: Cambridge.
16. E. Keehan, L. Karlsson, H.-O. Andrén, L.-E. Svensson, New developments with C–Mn–Ni high strength steel weld metals, Part B. Mechanical Properties, In Manuscript
17. K.W. Andrews, D. J. Dyson, S. R. Keown, Interpretation of Electron Diffraction Pat terns, 2nd Ed., Adam Hilger Ltd., London (1971).
18. J. W. Edington, Practical Electron Microscopy in Material Science, The Macmillan Press Ltd., London (1975)
19. http://cimesg1.epfl.ch/CIOL/ems.html